Journal of Mathematics and Statistics

Original Research Paper

Flow and Heat Transfer Profiles in a Square Channel with 45° V-Downstream Orifices

[1]Withada Jedsadaratanachai and [2]Amnart Boonloi

[1]Department of Mechanical Engineering, Faculty of Engineering, King Mongkut's Institute of Technology Ladkrabang, Bangkok 10520, Thailand
[2]Department of Mechanical Engineering Technology, College of Industrial Technology, King Mongkut's University of Technology North Bangkok, Bangkok 10800, Thailand

Article history
Received: 05-05-2016
Revised: 25-10-2016
Accepted: 15-11-2016

Corresponding Author:
Withada Jedsadaratanachai
Department of Mechanical Engineering, Faculty of Engineering, King Mongkut's Institute of Technology Ladkrabang, Bangkok 10520, Thailand
Email: kjwithad@kmitl.ac.th

Abstract: Flow and heat transfer profiles in a square channel heat exchanger inserted with 45° V-orifices are presented. The influences of Reynolds number (Re = 3000-10,000) and blockage ratio (BR = 0.05, 0.10, 0.15, 0.20 and 0.25) on periodic concepts are investigated numerically. The computational domain is solved with the finite volume method and SIMPLE algorithm. As the numerical results, the periodic profiles on flow and heat transfer are found when inserted the 45° V-orifices in the square duct. The configurations on flow and heat transfer in the heating section can separated into two sections; periodic profile and fully developed periodic profile. The patterns on flow and heat transfer are similar, but the values are not equal, called "periodic profiles", while the identical on both profiles and values, called "fully developed periodic profiles". In addition, the periodic structures depends on the parameters of the vortex generator, position in the channel and Reynolds number.

Keywords: Periodic Boundary, V-Orifice, Turbulent Flow, Numerical Investigation, Heat Exchanger

Introduction

Numerical investigation had been widely used to study the mechanisms in many engineering works such as strength of the materials, conduction of the materials, flow and heat transfer in the heat exchangers, aerodynamic of automotive parts, etc. The numerical validations and accurate setting of the computational domain are necessary for the numerical investigation. The time of solution and computational resource are important factors for the numerical study. For the numerical investigations on flow and heat transfer in the heat exchangers inserted with arrays of turbulators or vortex generators, the periodic boundary or periodic concept is always applied to the computational domain to save time for investigation. Many researchers had been compared between the flow and heat transfer profiles in the full length of the heating system with the periodic module. For examples, Jedsadaratanachai *et al.* (2011) created the computational domain of the square channel heat exchanger inserted with baffles by periodic boundary at the inlet and outlet of the domain. They gave the assumptions for the numerical investigation on the long heating system that the periodic structures occur due to the array of the baffle. They also compared between the results from full length of the heating section and periodic module on both flow and heat transfer. They reported that the fully developed periodic profiles are found around x/D = 7. Promvonge *et al.* (2012) applied the periodic boundary for inlet and outlet of the square channel heat exchanger placed with V-baffles. They found that the fully developed periodic profiles on flow and heat transfer are around x/D = 8 downstream of the entry. They also concluded that the periodic module of the computational model can save computational resource and time for investigation. The periodic boundary was applied for the computational domain of the heating or cooling sections inserted with various types of the turbulators or vortex generators (Jedsadaratanachai and Boonloi (2014; Jedsadaratanachai *et al.*, 2015; Boonloi and Jedsadaratanachai, 2015; Promvonge *et al.*, 2010;

Promthaisong *et al*., 2016). The computational domains were validated with the base case and experimental results. The researchers reported that the numerical results were found in excellence agreement with the correlations of the smooth channel/tube and the values from the experiments. They also concluded that the periodic modules had reliability to predict flow and heat transfer configurations in the heating systems.

The turbulators or vortex generators, which use to enhance the heat transfer rate and performance in the heat exchanger, have many types such as rib, baffle, wing, winglet, etc. Each type of the vortex generators gives different flow and heat transfer behaviors. The selection of the vortex generators is depended on the applications of the heat exchanger. Except from the types of the vortex generator, the parameter, placement and arrangement of the vortex generators are important variables that effect for the change of the flow and heat transfer mechanisms in the heating section. As preliminary study, the authors found that the V-shaped baffle/thin rib has high effectiveness for enhancing heat transfer rate and thermal performance, especially, V-downstream arrangement (V-tips point downstream). In the present work, the V-baffle is combined with the orifice plate called "V-orifice". The V-orifice may help to increase the strength of the flow in the heating system.

The heat exchanger inserted with the orifice shape had been reported by many researcher. Kongkaitpaiboon *et al*. (2010a) experimentally examined on convective heat transfer and pressure loss in a tube heat exchanger with circular-ring/orifice. The influences of the flow area (diameter ratio) and pitch ratios (*P*/*D*) were observed for turbulent regime, *Re* = 4000-20,000. They summarized that the enhancement of the heat transfer rate is around 57-195% higher than the baseline case. The heat transfer augmentations in the heat exchanger with conical-ring were presented (Yakut and Sahin, 2004; Yakut *et al*., 2004; Durmus, 2004; Eiamsa-ard and Promvonge, 2006a; 2006b; Promvonge and Eiamsa-ard, 2007a; 2007b; 2007c; 2007d; Kongkaitpaiboon *et al*., 2010a; Ozceyhan *et al*., 2008; Akansu, 2006; Kiml *et al*., 2003; 2004; Kongkaitpaiboon *et al*., 2010b). The researchers concluded that the flow area has high effect for the increment of the pressure loss in the heat exchanger.

The description of the periodic concepts on flow and heat transfer in the heating section inserted with V-orifice has rarely been reported. Therefore, the main objective of this work is to investigate the flow and heat transfer profiles in the square channel inserted with the vortex generators. The distances from the inlet for the appearances of the periodic and fully developed periodic profiles are considered. The 45° V-orifice with downstream arrangement is selected as the vortex generators. The effects of the blockage ratio (*BR* = 0.05, 0.10, 0.15, 0.20 and 0.25) and Reynolds number (*Re* = 3000-10,000) on periodic profiles are presented. The flow visualization and heat transfer mechanism in the test section inserted with array of V-orifice are stated. The numerical result from the periodic test is an important knowledge to improve the accuracy of the computational setting for the numerical investigation. The precise condition for the computational domain can help to increase reliability of the numerical investigation.

Numerical Method

The circular tube flow is solved by the continuity equation, Navier-Stokes equation and energy equation. The mathematical foundation and numerical method are referred by Promthaisong *et al*. (2016). The realizable *k*-ε model (Launder and Spalding (1974)) is selected for the current numerical solution:

$$\frac{\partial}{\partial t}(\rho k)+\frac{\partial}{\partial x_j}(\rho k u_j)=\frac{\partial}{\partial x_j}\left[\left(\mu+\frac{\mu_t}{\sigma_k}\right)\frac{\partial k}{\partial x_j}\right] + G_k + G_b - \rho\varepsilon + Y_M + S_k \tag{1}$$

and:

$$\frac{\partial}{\partial t}(\rho \varepsilon)+\frac{\partial}{\partial x_j}(\rho \varepsilon u_j)=\frac{\partial}{\partial x_j}\left[\left(\mu+\frac{\mu_t}{\sigma_\varepsilon}\right)\frac{\partial \varepsilon}{\partial x_j}\right] + \rho C_1 S\varepsilon + \rho C_2\frac{\varepsilon^2}{k+\sqrt{\upsilon\varepsilon}} + C_{1\varepsilon}\frac{\varepsilon}{k}C_{3\varepsilon}G_b + S_\varepsilon \tag{2}$$

where:

$$C_1 = \max\left[0.43, \frac{\eta}{\eta+5}\right], \eta = S\frac{k}{\varepsilon}, S=\sqrt{2S_{ij}S_{ij}} \tag{3}$$

The constant values are as follows:

$$C_{1\varepsilon}=1.44, C_2=1.9, \sigma_k=1.0, \sigma_\varepsilon=1.2 \tag{4}$$

The air velocity is calculated in term of Reynolds number bases on the hydraulic diameter of the square channel (*D* = *H*) as follow:

$$\mathrm{Re}=\frac{\rho u_0 D}{\mu} \tag{5}$$

The pressure drop across the test section is measured and reported in term of friction factor:

$$f=\frac{(\Delta P/L)D_h}{2\rho\bar{u}^2} \tag{6}$$

The local Nusselt number and the average Nusselt number are representative for heat transfer rate of the heating section:

$$Nu_x = \frac{h_x D_h}{k} \tag{7}$$

$$Nu = \frac{1}{A}\int Nu_x dA \tag{8}$$

Channel Geometry, Boundary Condition and Assumption

Figure 1 presents the square channel heat exchanger inserted with the V-orifices, while the details and parameters of the V-orifice are depicted in the Fig. 2. The square channel height is set around 0.05 m. The orifice height presents by b, while the ratio between b and H is known as the blockage ratio or b/H (BR). The flow attack angle and pitch spacing ratio of the V-orifice are fixed at 45° and 1, respectively. The V-Downstream arrangement or flow direction (V-tip indicating downstream) is selected for the present study.

The entry and exit regions are around 10H, while the test section is around 12H (12 modules). The velocity inlet and pressure outlet are set for inlet and outlet of the computational domain. The uniform heat flux around 600 W/m^2 is applied for the all sides of the test section. The V-orifices are assumed to be an insulator. No slip wall condition is set for the square channel walls.

The flow is turbulent and incompressible. The steady condition is set for both flow and heat transfer. The convective heat transfer is considered. The natural convection and radiation heat transfer are disregarded. The body force and viscous dissipation are ignored. The air as the tested fluid is set with constant fluid properties at the average bulk temperature.

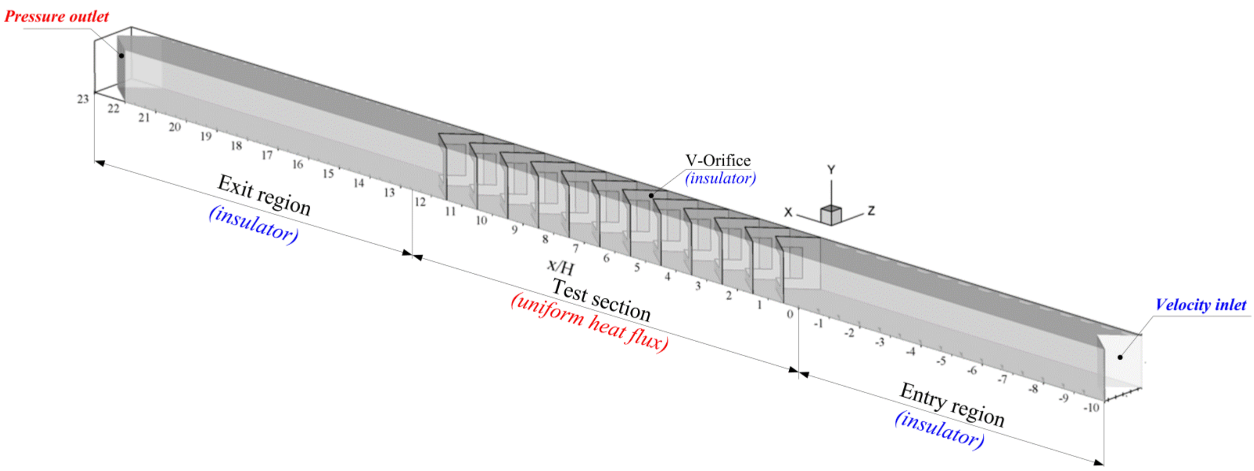

Fig. 1. Square channel heat exchanger inserted with V-orifices

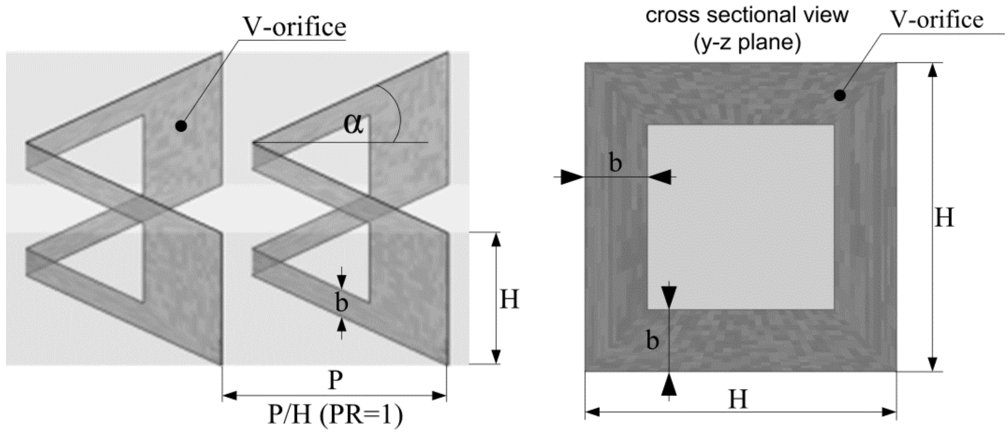

Fig. 2. Details of V-orifices

Results and Discussion

The numerical outcomes of the test section inserted with array of V-orifice can separate into three sections: Numerical validation, influence of the Reynolds number and influence of the blockage ratio. The validation part helps to check the accuracy of the computational domain and boundary condition and helps to enhance the reliable of the numerical results.

Validation of the Computational Domain

The Nusselt number and friction factor of the smooth square channel are compared with the values from the correlations (Incropera and Dewitt, 2006). The acceptable range of the deviations on both heat transfer and friction loss should be within ±10%. As the result, the numerical and correlation results are in similar trends. The deviations of the Nusselt number and friction loss are around 2.5 and 8%, respectively, as Fig. 3.

The polyhedral mesh is selected for the computational domain. The grid independence is reported in Fig. 4. As the figure, the increasing grid cell from 640000 to 800000 has no advantage for the numerical results. Therefore, the grid around 640000 is selected for all cases of the present works. As above, it can be concluded that the computational domain has dependability to calculate the mechanisms in the square channel heat exchanger inserted with the V-orifices.

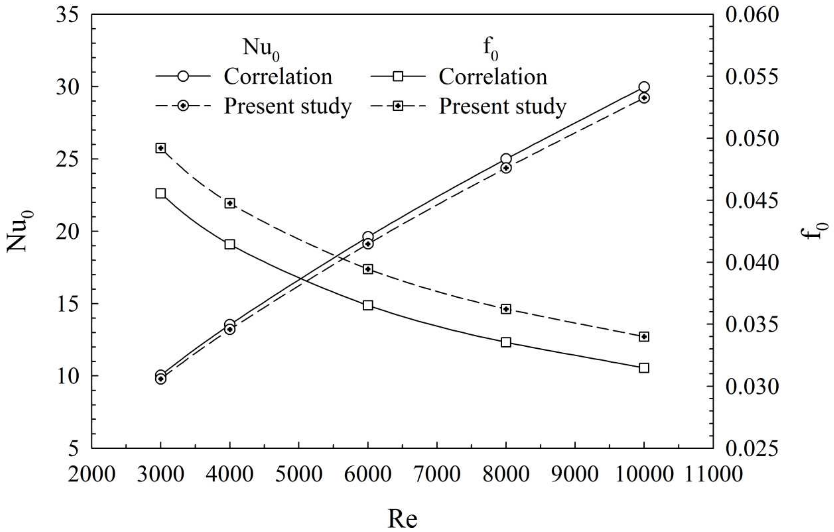

Fig. 3. Validations of the smooth square channel

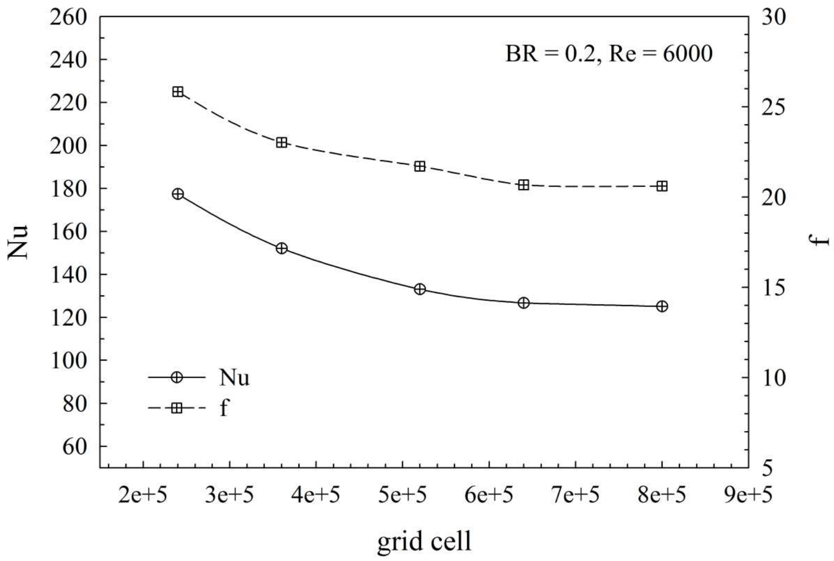

Fig. 4. Grid independence

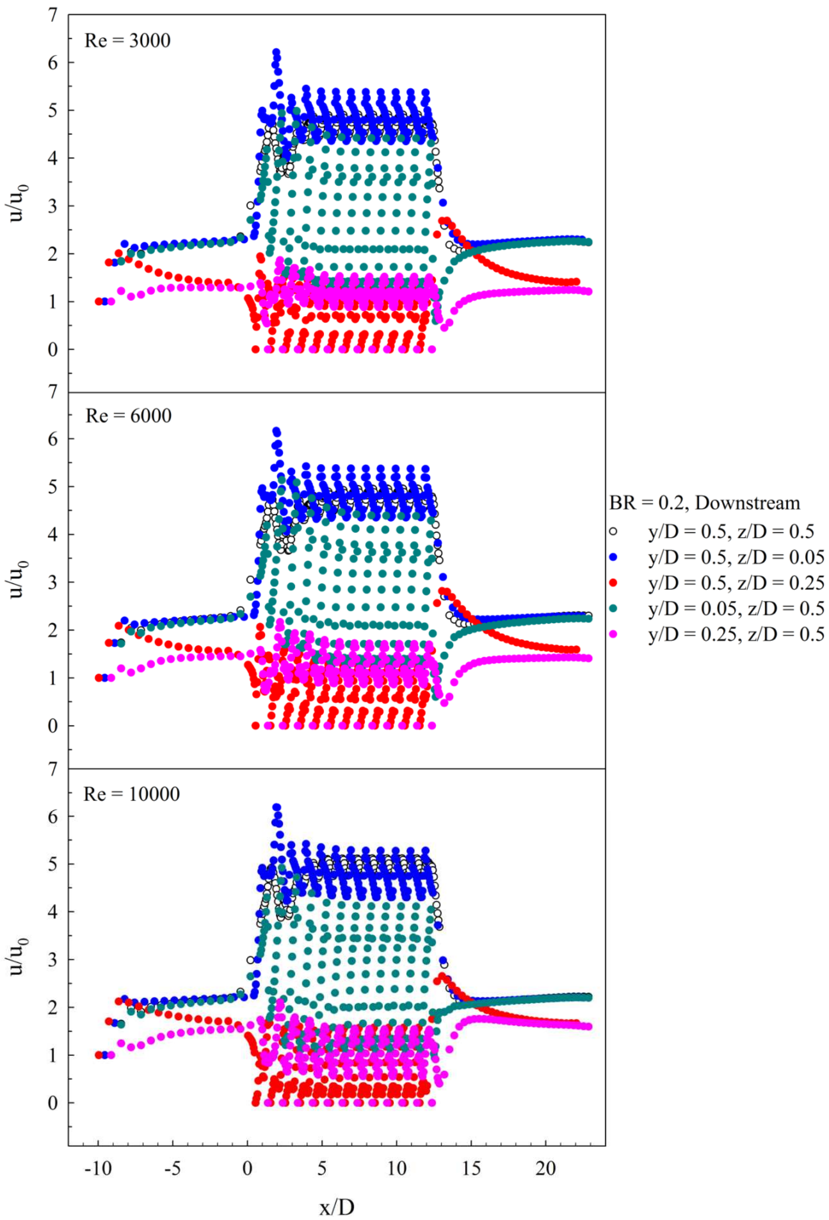

Fig. 5. u/u_0 Vs x/D for V-orifice with $BR = 0.2$ at various Re and positions

Effect of Reynolds Number

Figure 5 presents the relations of the u/u_0 with x/D for Reynolds number of 3000, 6000 and 10,000 at various y/D and z/D values for $BR = 0.2$. The flow profiles in the square channel heat exchanger can divided into two zones for all Reynolds numbers. The similar flow profiles with different velocity values called "periodic flow profile", which are found in the upstream regime. The flow profiles and values show identically, called "fully developed periodic flow profile", which are detected next from the periodic flow profiles. At the middle of the channel ($y/D = z/D = 0.5$), periodic flow profiles appear around $x/D = 2$ (2rd module) for all Reynolds numbers, while the fully developed periodic flow profiles are found at $x/D = 6$-7 (6th-7th module). Considering at $Re = 10,000$, it is found that the fully developed periodic profile appear quickly around one module when measuring at close to the channel walls ($y/D = 0.5$, $z/D = 0.05$ and $y/D = 0.05$, $z/D = 0.5$). The similar trend is found for all the Reynolds number. Figure 6 and 7 report the variations of the u/u_0 with y/D and z/D, respectively, at various x/D values for $BR = 0.2$ and $BR = 3000$, 6000 and 10,000. The periodic flow profiles are detected around $x/D = 1.5$, while the fully developed periodic flow profiles are found around $x/D =$

5.5-7.5. Figure 8 plots the streamlines in transverse planes at various x/D and Re values for $BR = 0.2$. The developing flows are found in $x/D = 0.5$-2.5, while the fully developed flows appear at $x/D = 3.5$ for all cases. In conclusion, the Reynolds number has slightly effect for the periodic flow structure in the heating section.

Figure 9 present the Nu/Nu_0 versus x/D for $BR = 0.2$ at various Re and positions. The periodic heat transfer profiles are separated into two regimes; periodic heat transfer and fully developed periodic heat transfer, similarly as the flow structure. The periodic heat transfer profile means that the configuration of the Nusselt number is similarly, while the fully developed periodic heat transfer profile means that the both configuration and value of the Nusselt number are identically. The periodic heat transfer profiles are found around $x/D = 3$, while the fully developed periodic heat transfer profiles are detected around $x/D = 4$-6. The heat transfer rate in term of the local Nusselt number distributions on the channel walls are depicted in Fig. 10. The identical heat transfer profiles are found from the second module to the last module. The rise of the Reynolds number has slightly effect for the appearance of the fully developed periodic profiles on both flow and heat transfer profiles.

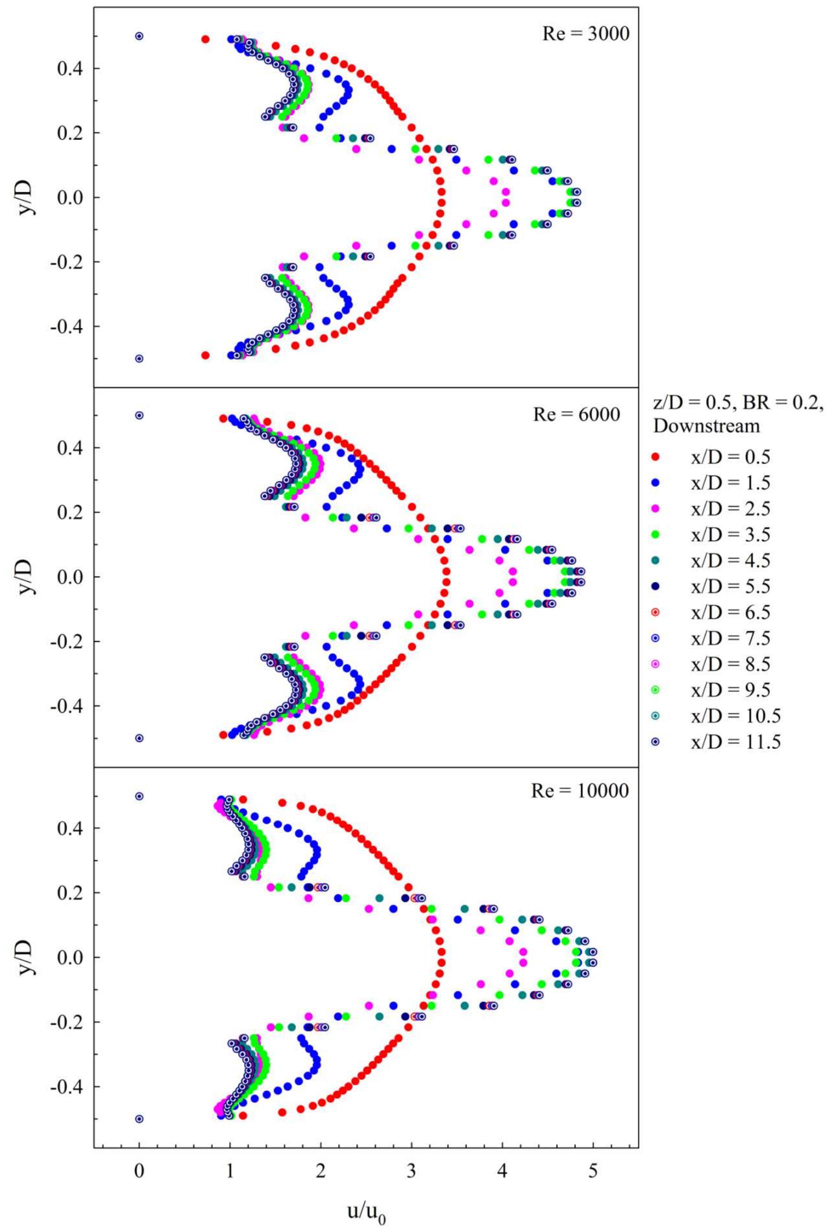

Fig. 6. y/D Vs u/u_0 for V-orifice with $BR = 0.2$ at various Re and positions

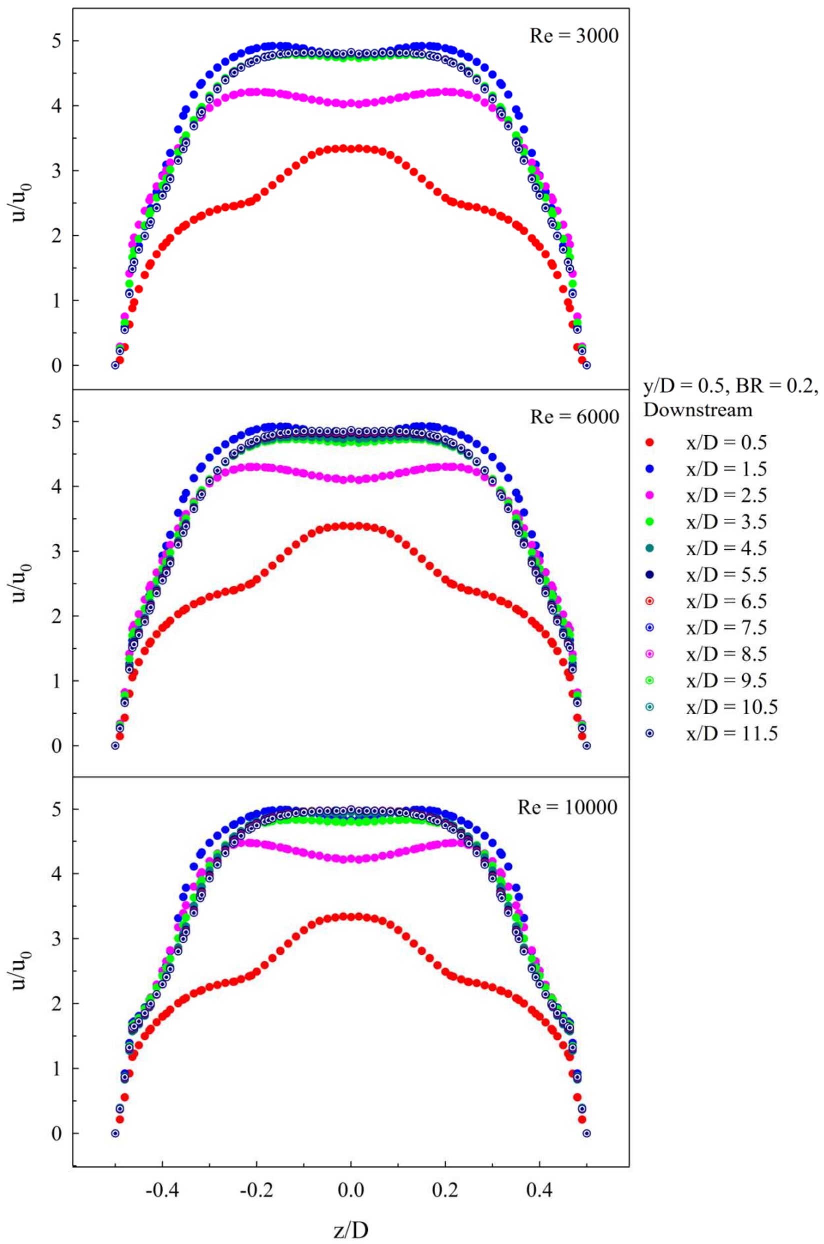

Fig. 7. u/u_0 vs z/D for V-orifice with *BR* = 0.2 at various *Re* and positions

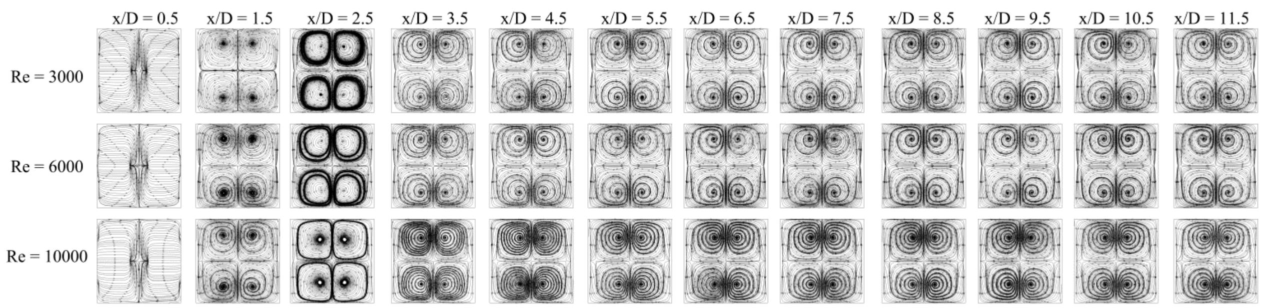

Fig. 8. Streamlines in y-z planes for V-orifice with *BR* = 0.2 at various *Re* and positions

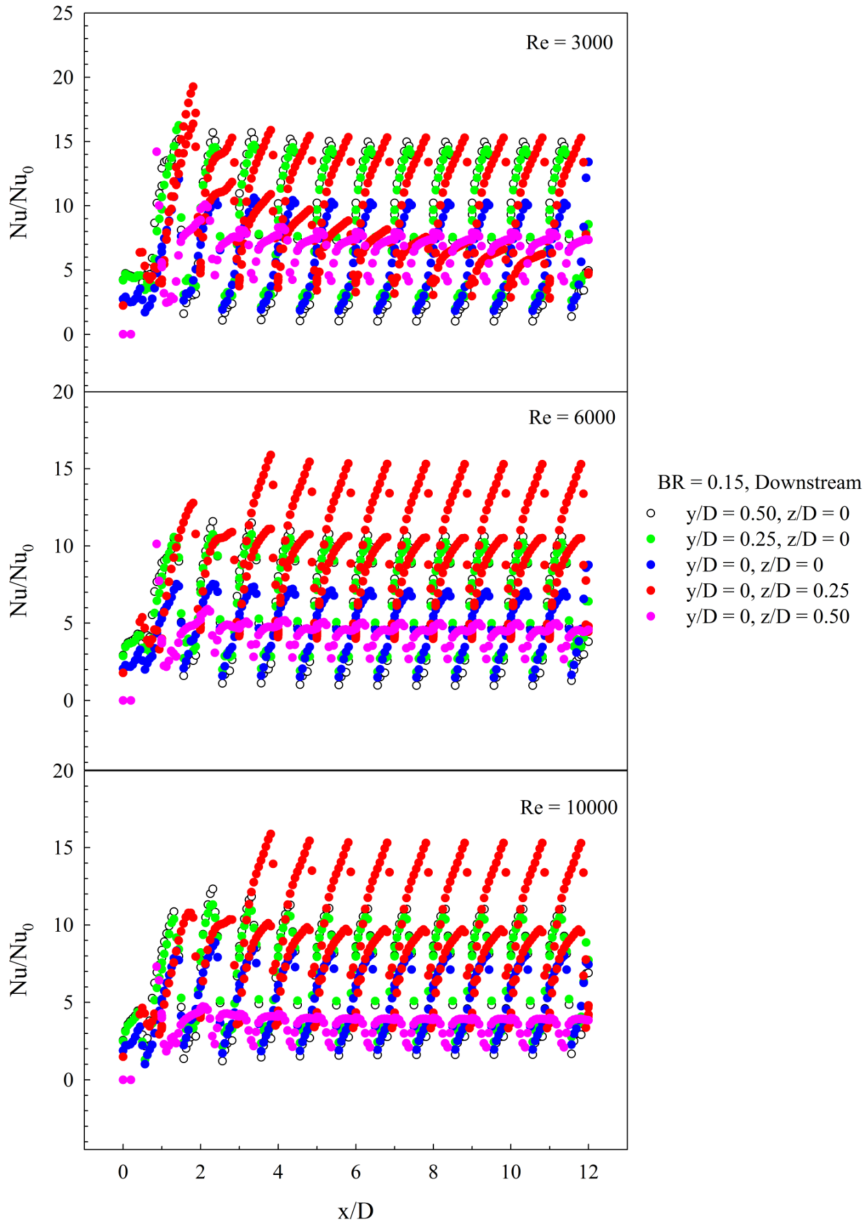

Fig. 9. Nu/Nu_0 vs x/D for V-orifice with BR = 0.15 at various Re and positions

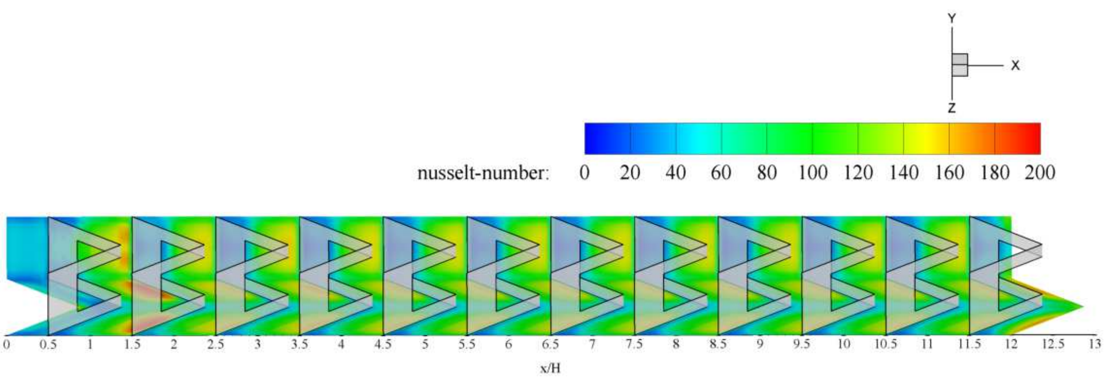

(a)

DOI: 10.3844/jmssp.2016.277.289

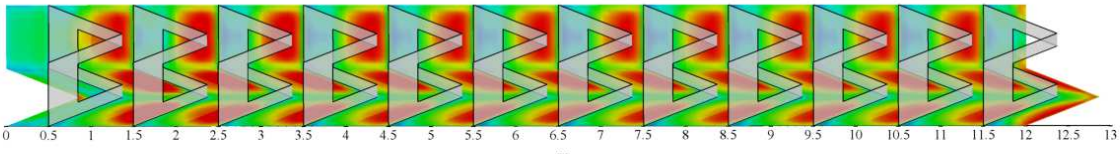

(b)

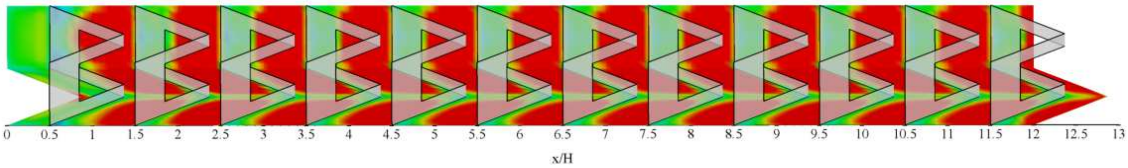

(c)

Fig. 10 Nu_x contours for V-orifice at BR = 0.15 of (a) Re = 3000, (b) Re = 6000 and (c) Re =10000

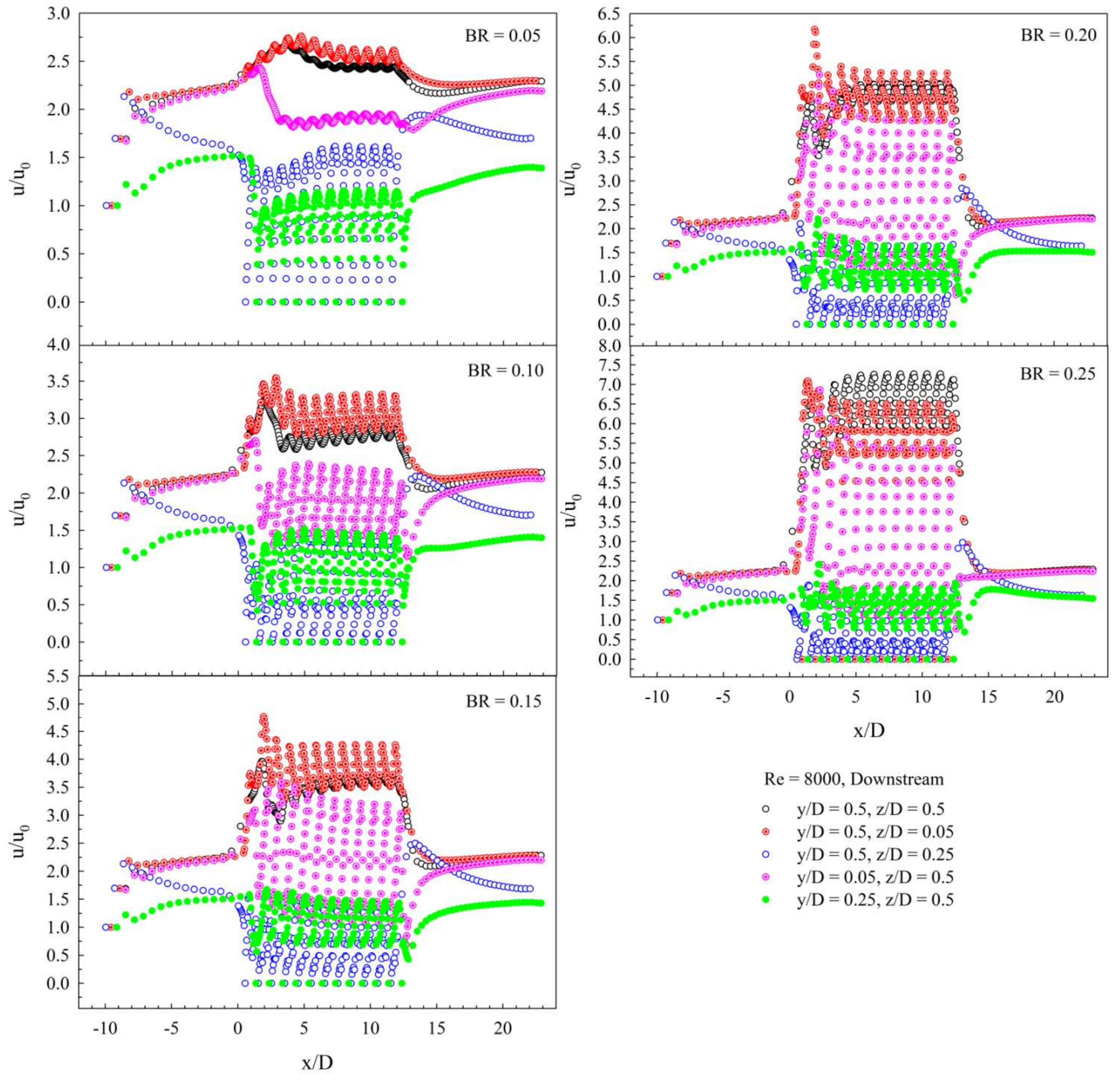

Fig. 11. u/u_0 Vs x/D for V-orifice with Re = 8000 at various BRs and positions

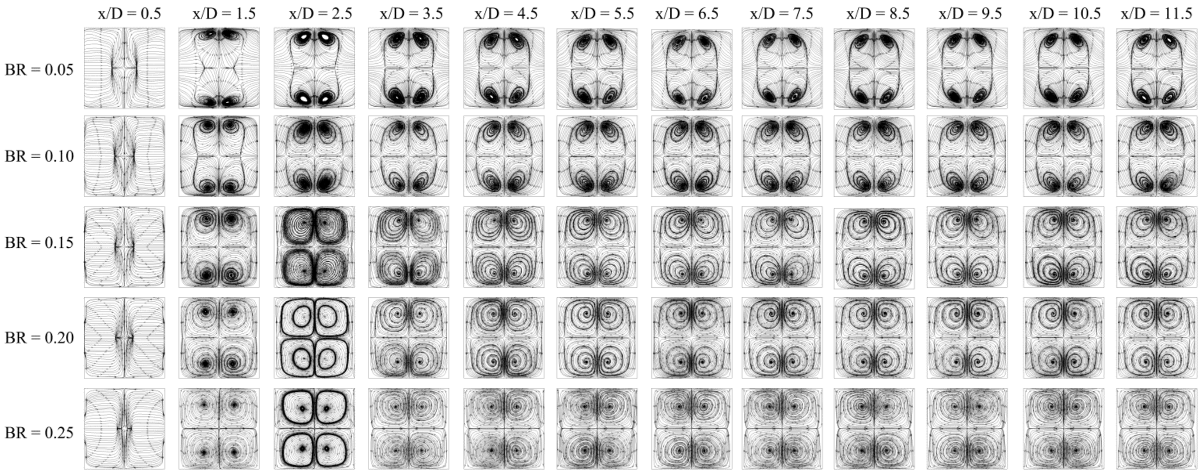

Fig. 12. Streamlines in *y-z* planes for V-orifice with *Re* = 8000 at various *BR*s and positions

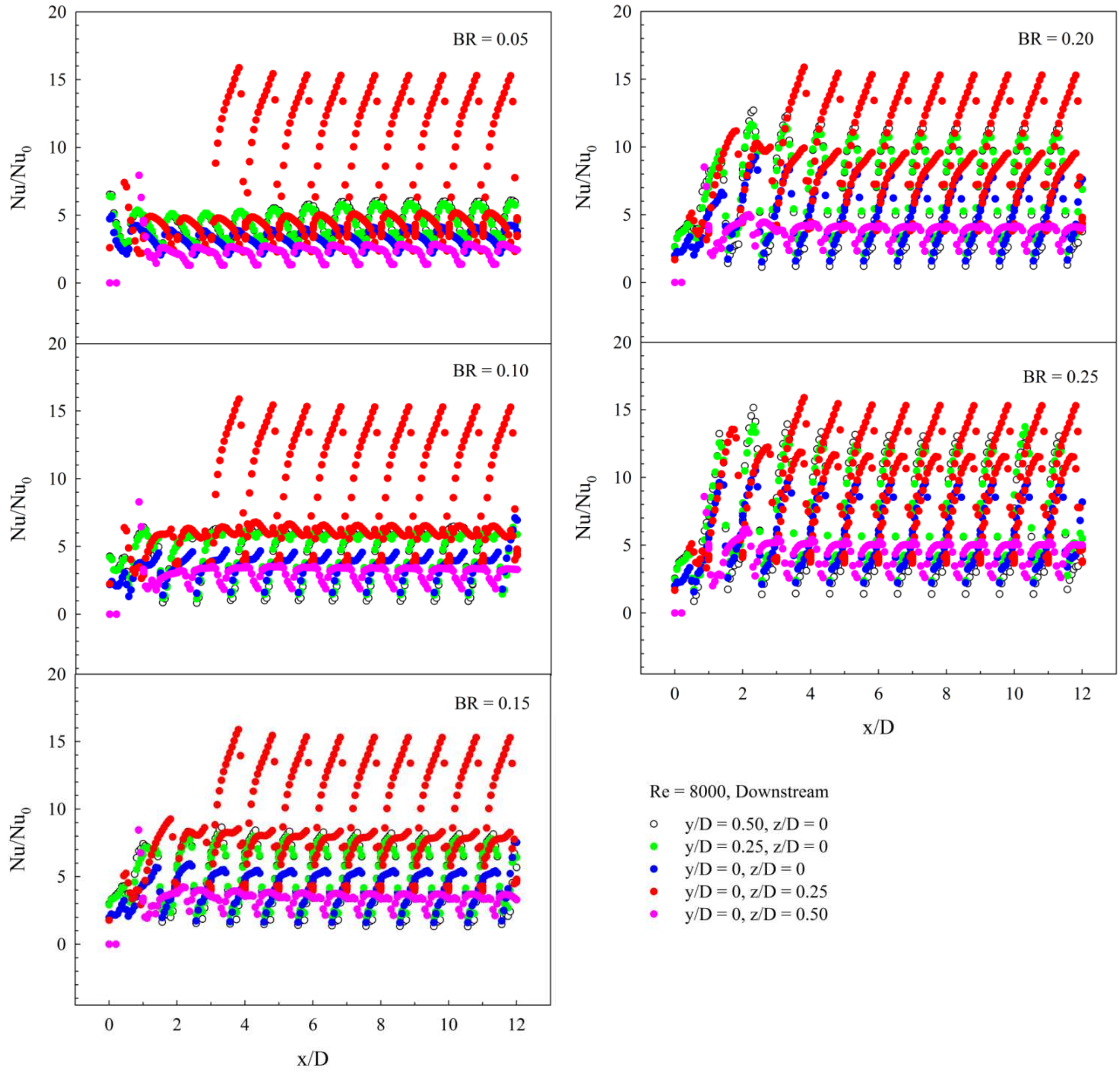

Fig. 13. Nu/Nu_0 Vs x/D for V-orifice with *Re* = 8000 at various *BR*s and positions

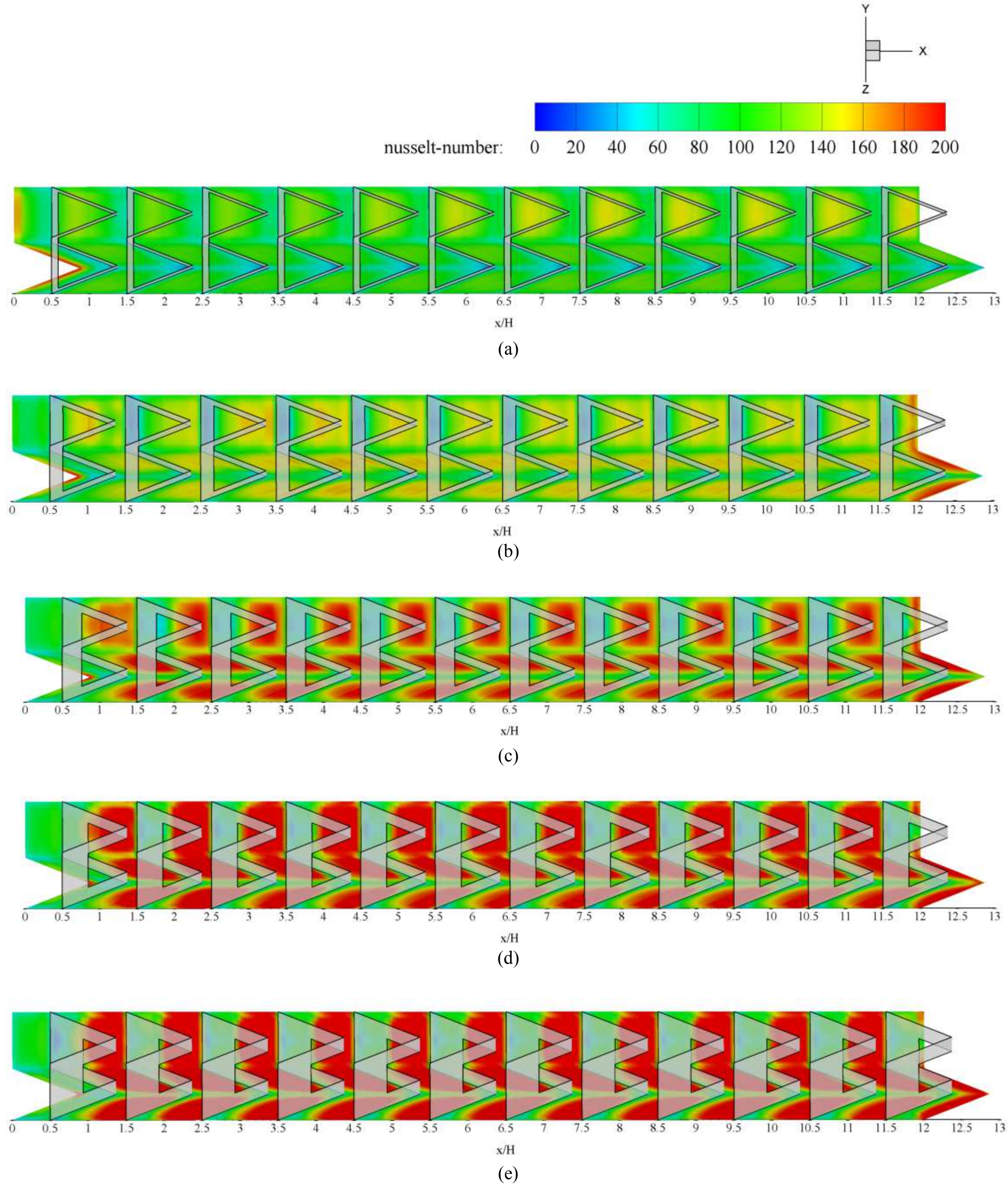

Fig. 14. Nu_x contours for V-orifice at *Re* = 8000 of (a) *BR* = 0.05, (b) *BR* = 0.10, (c) *BR* = 0.15, (d) *BR* = 0.20 and (e) *BR* = 0.25

Effect of Blockage Ratio

Figure 11 illustrates the variations of the u/u_0 with the x/H at various *BR*s and positions for *Re* = 8000. The periodic flow and fully developed periodic flow profiles are detected in all *BR*s. The rise of the *BR* provides higher velocity values. The *BR* = 0.25 gives the highest velocity values, while the *BR* = 0.05 performs the opposite results. The periodic flow profiles are found around x/D = 2 in all *BR*s, while the fully developed periodic flow profiles are detected around x/D = 7-8, 5-7, 5-7, 4-6 and 4-5 for the *BR* = 0.05, 0.10, 0.15, 0.20 and 0.25, respectively, depended on the position in the channel. The increasing *BR* leads to speed up of the fully developed periodic flow profiles. The *BR* = 0.25 gives the fastest trend of the fully developed periodic flow profiles, while the *BR* = 0.05 provides the reverse trend. In addition, the positions that close to the channel walls (y/D = 0.5, z/D = 0.05 and y/D = 0.05, z/D = 0.5) occurs the fully developed periodic flow rapidly in comparison with the other regimes. The flow topology in term of the streamlines in *y*-*z* planes is shown in Fig. 12. As the figure, the developing flow profiles are found at x/D = 0.5, 1.5 and 2.5, after that the flow configurations seem to be similar in all planes. In conclusion, the *BR* has significantly effect for the periodic and fully developed periodic flow profiles. The large flow blockage ratio (low flow area) leads to speed up of the fully developed periodic flow profile. Figure 13 presents the variations of the Nu_x/Nu_0 with x/D at various *BR*s and positions. The numerical trends of the heat transfer profile are similarly as the flow profile that the periodic heat transfer profiles are found around x/D = 2-3, while the fully developed periodic heat transfer profile are found around x/D = 4-8. The local Nusselt number distributions on the channel walls with various *BR*s are reports as Fig. 14. The fully developed periodic heat transfer profiles are found rapidly when reducing flow area in the square channel heat exchanger.

Conclusion

The numerical investigations on periodic concepts of flow and heat transfer in the heating section with V-orifice are examined. The effects of blockage ratio and Reynolds number are considered. The scope of this work is fixed for the turbulent regime, *Re* = 3000-10,000, with the blockage ratio, *BR* = 0.05-0.25. The numerical results are concluded as follows:

The flow and heat transfer profiles are divided into two zones; periodic profile and fully develop periodic profile. The periodic profile is found around module (while the fully developed periodic profile is detected around 4th-8th module.

The accelerations of the fully developed periodic profiles on both flow and heat transfer are found quickly when rising the Reynolds number and blockage ratio.

The periodic boundary can apply for the computational domain of the heating or cooling system that installed with the arrays of the vortex generators. The periodic concept helps to save time to investigation with remain high accuracy results. Moreover, the periodic concept also helps to conserve the computer resource.

The periodic structures should be check for different shape of the vortex generators. The accurate setting for the computational model can help to enhance reliability of the numerical result.

Acknowledgement

The authors would like to acknowledge Assoc. Prof. Dr. Pongjet Promvonge for suggestions.

Funding Information

The research was sponsored by King Mongkut's University of Technology North Bangkok and King Mongkut's Institute of Technology Ladkrabang.

Author's Contributions

Withada Jedsadaratanachai: Participated in designing a research mechanicm scheme from beginning to end, writing manuscript.

Amnart Boonloi: Participated in writing of the manuscript, assessing and estimating model parameters.

Ethics

This article is original and contains unpublished material. The corresponding author confirms that all of the other authors have read and approved the manuscript and no ethical issues involved."

References

Akansu, S.O., 2006. Heat transfers and pressure drops for porous-ring turbulators in a circular pipe. Applied Energy, 83: 280-298. DOI: 10.1016/j.apenergy.2005.02.003

Boonloi, A. and W. Jedsadaratanachai, 2015. Turbulent forced convection in a heat exchanger square channel with wavy-ribs vortex generator. Chinese J. Chem. Eng., 23: 1256-1265. DOI: 10.1016/j.cjche.2015.04.001

Durmus, A., 2004. Heat transfer and exergy loss in cut out conical turbulators. Energy Convers. Manage., 45: 785-796. DOI: 10.1016/S0196-8904(03)00186-9

Eiamsa-ard, S. and P. Promvonge, 2006a. Effect of V-nozzle inserts and snail with free spacing entry on heat transfer in a heat exchanger. J. Energy Heat Mass Transfer, 28: 225-239.

Eiamsa-ard, S. and P. Promvonge, 2006b. Experimental investigation of heat transfer and friction characteristics in a circular tube fitted with V-nozzle turbulators. Int. Commun. Heat Mass Transfer, 33: 591-600. DOI: 10.1016/j.icheatmasstransfer.2006.02.022

Incropera, F. and P.D. Dewitt, 2006. Introduction to Heat Transfer. 3rd Edn., John Wiley and Sons Inc.

Jedsadaratanachai, W. and A. Boonloi, 2014. Effects of blockage ratio and pitch ratio on thermal performance in a square channel with 30° double V-baffles. Case Stud. Thermal Eng., 4: 118-128. DOI: 10.1016/j.csite.2014.08.002

Jedsadaratanachai, W., N. Jayranaiwachira and P. Promvonge, 2015. 3D numerical study on flow structure and heat transfer in a circular tube with V-baffles. Chinese J. Chem. Eng., 23: 342-349. DOI: 10.1016/j.cjche.2014.11.006

Jedsadaratanachai, W., S. Suwannapan and P. Promvonge, 2011. Numerical study of laminar heat transfer in baffled square channel with various pitches. Energy Proc., 9: 630-642. DOI: 10.1016/j.egypro.2011.09.073

Kiml, R., A. Magda, S. Mochizuki and A. Murata, 2004. Rib-induced secondary flow effects on local circumferential heat transfer distribution inside a circular rib-roughened tube. Int. J. Heat Mass Transfer, 47: 1403-1412. DOI: 10.1016/j.ijheatmasstransfer.2003.09.026

Kiml, R., S. Mochizuki, A. Murata and V. Stoica, 2003. Effects of rib-induced secondary flow on heat transfer augmentation inside a circular tube. J. Enhanced Heat Transfer, 10: 9-20. DOI: 10.1615/JEnhHeatTransf.v10.i1.20

Kongkaitpaiboon, V., K. Nanan and S. Eiamsa-ard, 2010a. Experimental investigation of heat transfer and turbulent flow friction in a tube fitted with perforated conical rings. Int. Commun. Heat Mass Transfer, 37: 560-567. DOI: 10.1016/j.icheatmasstransfer.2009.12.015

Kongkaitpaiboon, V., K. Nanan and S. Eiamsa-ard, 2010b. Experimental investigation of convective heat transfer and pressure loss in a round tube fitted with circular-ring turbulators. Int. Commun. Heat Mass Transfer, 37: 568-574. DOI: 10.1016/j.icheatmasstransfer.2009.12.016

Launder, B.E. and D.B. Spalding, 1974. The numerical computation of turbulent flows. Comput. Meth. Applied Mechan. Eng., 3: 269-289. DOI: 10.1016/0045-7825(74)90029-2

Ozceyhan, V., S. Gunes, O. Buyukalaca and N. Altuntop, 2008. Heat transfer enhancement in a tube using circular cross sectional rings separated from wall. Applied Energy, 85: 988-1001. DOI: 10.1016/j.apenergy.2008.02.007

Promthaisong, P., P. Eiamsa-ard, W. Jedsadaratanachai and S. Eiamsa-ard, 2016. Turbulent heat transfer and pressure loss in a square channel with discrete broken V-rib turbulators. J. Hydrodynam., 28: 275-283. DOI: 10.1016/S1001-6058(16)60629-7

Promvonge, P. and S. Eiamsa-ard, 2007a. Heat transfer and turbulent flow friction in a circular tube fitted with conical-nozzle turbulators. Int. Commun. Heat Mass Transfer, 34: 72-82. DOI: 10.1016/j.icheatmasstransfer.2006.08.003

Promvonge, P. and S. Eiamsa-ard, 2007b. Heat transfer augmentation in a circular tube using V-nozzle turbulator inserts and snail entry. Exp. Thermal Fluid Sci., 32: 332-340. DOI: 10.1016/j.expthermflusci.2007.04.010

Promvonge, P. and S. Eiamsa-ard, 2007c. Heat transfer behaviors in a tube with combined conical-ring and twisted-tape insert. Int. Commun. Heat Mass Transfer, 34: 849-859. DOI: 10.1016/j.icheatmasstransfer.2007.03.019

Promvonge, P. and S. Eiamsa-ard, 2007d. Heat transfer in a circular tube fitted with free spacing snail entry and conical-nozzle turbulators. Int. Commun. Heat Mass Transfer, 34: 838-848. DOI: 10.1016/j.icheatmasstransfer.2007.03.020

Promvonge, P., W. Jedsadaratanachai and S. Kwankaomeng, 2010. Numerical study of laminar flow and heat transfer in square channel with 30° inline angled baffle turbulators. Applied Thermal Eng., 30: 1292-1303. DOI: 10.1016/j.applthermaleng.2010.02.014

Promvonge, P., W. Jedsadaratanachai, S. Kwankaomeng and C. Thianpong, 2012. 3D simulation of laminar flow and heat transfer in V-baffled square channel. Int. Commun. Heat Mass Transfer, 39: 85-93. DOI: 10.1016/j.icheatmasstransfer.2011.09.004

Yakut, K. and B. Sahin, 2004. Flow-induced vibration analysis of conical-rings used of heat transfer enhancement in heat exchanger. Applied Energy, 78: 273-288. DOI: 10.1016/j.apenergy.2003.09.001

Yakut, K., B. Sahin, S. Canbazoglu, 2004. Performance and flow-induced vibration characteristics for conical-ring turbulators. Applied Energy, 79: 65-76. DOI: 10.1016/j.apenergy.2003.11.002

Nomenclature

BR	flow blockage ratio (= b/H)
b	orifice height, m
D	hydraulic diameter of square channel (= H)
f	friction factor
h	convective heat transfer coefficient, W m^{-2} K^{-1}
k	thermal conductivity, W m^{-1} K^{-1}
Nu	Nusselt number (= hD/k)
P	orifice pitch
p	static pressure, Pa
Pr	Prandtl number (Pr = 0.707)
PR	pitch or spacing ratio (=P/H)
Re	Reynolds number $\left(= \rho\bar{u}D/\mu\right)$
T	temperature, K
u_i	velocity in x_i-direction, m s^{-1}
$\bar{u}$	mean velocity in channel, m s^{-1}
Greek letter	
μ	dynamic viscosity, kg $s^{-1}m^{-1}$
α	angle of attack, degree
ρ	density, kg m^{-3}